8th U. S. National Combustion Meeting
Organized by the Western States Section of the Combustion Institute
and hosted by the University of Utah
May 19-22, 2013

The Effects of Fuel Type and Geometry on Emissions and Efficiency of Natural Draft Semi-Gasifier Biomass Cookstoves

Jessica Tryner Anthony J. Marchese Bryan D. Willson

Department of Mechanical Engineering, Colorado State University, Fort Collins, CO

Approximately half of the world's population uses solid biomass fuel for cooking. The resulting exposure to carbon monoxide (CO) and particulate matter (PM) emissions leads to increased risk of acute CO poisoning, cardiovascular disease, and respiratory ailments. Although some existing improved cookstoves reduce emissions substantially in comparison to a three stone fire or traditional stove, health studies suggest that greater reductions are needed. To quantify the emissions reductions and efficiency increases necessary for household cookstoves to be considered "improved", the ISO recently established a tiered rating system (modeled after the EPA diesel engine standards) in which Tier 4 represents the highest level of emissions and efficiency standards. Semi-gasifier cookstoves, which burn solid biomass fuel in a two-stage process in which the solid fuel is first gasified, are a promising means of achieving Tier 4 standards. In this study, five different configurations of natural draft, semi-gasifier cookstoves were tested with two different biomass fuels (corn cobs and wood pellets) to assess the effects of stove design and fuel type on performance. The Emissions and Performance Test Protocol was used to quantify performance in terms of CO emissions, PM emissions, and heat transfer efficiency (HTE) under high-power operating conditions. Each stove was instrumented with 17 to 24 type K thermocouples to monitor the combustion process and to collect temperature data that was input into an energy balance model. The energy balance model was then used to determine the major sources of efficiency loss. Although all of the configurations were based on the same operating principle, emissions varied substantially with stove geometry and fuel type. Overall HTE and the largest sources of efficiency loss also varied among the configurations. The maximum HTE achieved was 38%. The minimum CO and PM emissions achieved were 0.6 g and 48 mg per MJ of energy delivered to the cooking pot (MJ_d), respectively. These results meet Tier 3 standards for high-power emissions and efficiency and suggest that development of a natural draft semi-gasifier cookstove that meets Tier 4 standards (HTE > 45%, CO < 8 g/MJ_d, PM < 41 mg/MJ_d) is possible.

1. Introduction

Fifty percent of the global population is estimated to rely on the combustion of solid biomass fuel to fulfill some or all of their household energy needs (Rehfuess et al., 2006). The majority of this population cooks using simple stoves that are fueled by solid biomass and characterized by inefficient combustion. Public health researchers have linked exposure to the carbon monoxide (CO) and particulate matter (PM) emissions from incomplete combustion of solid biomass to numerous health effects such as acute lower respiratory infections and chronic obstructive pulmonary disease (Bruce et al., 2006). Some have suggested that a transition to affordable liquid or gaseous fuels for indoor cooking would be necessary to completely eliminate these health impacts (Goldemberg et al., 2004). However, even if a transition to liquid or gaseous fuels is ultimately necessary, such a transition would take many years to accomplish given the size and geographic distribution of the affected population. Consequently, a substantial fraction of the global population is expected to continue cooking with solid biomass fuel for the foreseeable future (Rehfuess et al., 2006).

In recent years, designers of household cookstoves have focused on improving efficiency and reducing emissions to mitigate the health impacts associated with the use of solid biomass fuel. For example, improved rocket elbow cookstoves have been shown to reduce emissions by 50 to 60 percent compared to a three-stone fire (Jetter and Kariher, 2009). However, ongoing public health research is expected to reveal that greater emissions reductions are needed to substantially reduce health risks (Smith and Peel, 2010). Semi-gasifier cookstoves are considered to be the lowest-emitting type of solid biomass cookstove (Jetter and Kariher, 2009, Smith, 2010).

Most of the semi-gasifier cookstoves that have been developed utilize the top-lit up-draft (TLUD) design (see Figure 1) (Anderson et al., 2007). In the TLUD design, solid fuel is batch fed into the combustion chamber and ignited from the top. Consumption of the fuel proceeds downward (Reed and Larson, 1996). A primary air source that enters at the bottom of the fuel bed results in partial oxidation of the fuel into CO, H_2, hydrocarbons, CO_2, and H_2O in the primary combustion zone. The hot char bed above the primary combustion zone reduces some of the CO_2 and H_2O produced in the primary combustion zone back to CO and H_2 (Quaak et al., 1999). A secondary air source, which is preheated by the walls of the combustion chamber, is then mixed with the combustible gases leaving the char zone to form the secondary combustion zone (Reed and Larson, 1996). Primary and secondary airflow can be driven externally (e.g. by a fan or blower) or buoyantly (via natural convection) (Smith and Balakrishnan, 2009). A stove in which airflow is driven externally is referred to as a "forced air" cookstove and a stove in which airflow is driven buoyantly is referred to as a "natural draft" cookstove. Burning the combustible gases in a location that is separate from the solid fuel bed enables better mixing of the gases with air and, consequently, more complete combustion (Anderson et al., 2007).

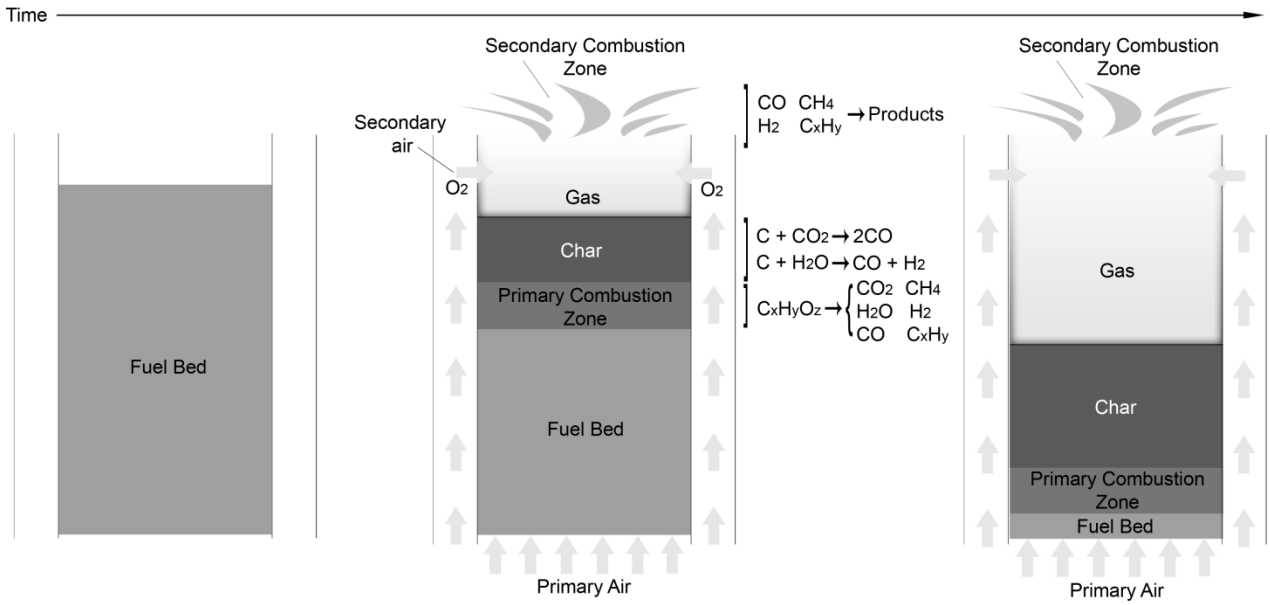

Figure 1. Schematic of top-lit up-draft (TLUD) semi-gasifier cookstove operation.

In this study, five different configurations of natural draft TLUD semi-gasifier household cookstoves were tested using two different fuels to determine how changes in stove design, fuel type, and operating procedure affected performance in terms of efficiency, carbon monoxide (CO) emissions, and particulate matter (PM_{10}) emissions. Forced-air semi-gasifier cookstoves have been shown to reduce CO and PM emissions by 90% relative to a three-stone fire in laboratory studies (Jetter and Kariher, 2009, MacCarty et al., 2010). However, previous work has suggested that natural draft semi-gasifier cookstoves typically do not perform as well as forced air semi-gasifier cookstoves (Smith and Balakrishnan, 2009, MacCarty et al., 2010, Kar et al., 2012).

The results of the present study suggest that natural draft TLUD semi-gasifier cookstoves can achieve relatively high efficiencies and substantial emissions reductions with careful design and selection of fuel type. The test results were also used to conduct an overall energy balance for each design configuration/fuel type combination to determine the sources of energy losses and opportunities for efficiency enhancement. Although the results are encouraging regarding the potential for reduced emissions and increased efficiency from TLUD semi-gasifier cookstoves under controlled operating conditions, the experimental results also clearly demonstrate a correlation between transient operation (such as adding volatile fuel to a hot char bed) and spikes in CO emissions.

2. Methods

The procedure and equipment used to measure the efficiency of and emissions from each stove, as well as the equations used to complete the calculations used in the thermodynamic energy balance are described below.

2.1 Test Protocol

The Emissions and Performance Test Protocol (EPTP), which is a modified version of the water boiling test (WBT), was used for all experiments reported in this study. The WBT is the most common test used to evaluate cookstove performance in the laboratory and is described in several studies on cookstove performance (Jetter and Kariher, 2009, MacCarty et al., 2010). The EPTP was created to reduce variability between test replicates without altering the general results of the WBT (L'Orange et al., 2012). A manual containing a detailed description of the EPTP test protocol is available for download online (DeFoort et al., 2010). It should be noted that, in the present study, only the "cold start" phase of the EPTP test protocol, in which 5 L of water is brought from 15°C to 90°C with the stove body starting out at room temperature, was employed. All tests were conducted in Fort Collins, CO, at an elevation of approximately 1500 m, where water boils at 95°C.

2.2 Testing Equipment

Tests were conducted in a fume hood with a 1.2 m square cross-section and a height of 4.3 m. The air flow rate through the hood was 6 m^3/min. The cross sectional area of the hood and the air flow rate were designed such that they do not affect the airflow through the stove (L'Orange et al., 2012). High efficiency particle air (HEPA) filters installed on the air inlet locations at the base of the fume hood prevented particulate matter in the ambient air from entering the hood. Exhaust gases were transported from the top of the hood to emissions analyzers by a 12.7 cm diameter pipe.

Total mass emissions of particulate matter with an aerodynamic diameter of less than 10μm (PM_{10}) were measured gravimetrically as described by L'Orange et al. (2012). Particulate matter was collected on Teflon filters that were pre- and post-weighed on a Mettler Toledo MX5 microbalance (Mettler-Toledo, LLC, Columbus, OH, USA). The limit of detection (LOD) and limit of quantification (LOQ) for these measurements were 16 μg and 55 μg, respectively. All PM mass emissions measurements were found to be above the LOQ with the exception of one measurement of 53 μg.

CO emissions were measured with Testo 335 and Testo 350 flue gas analyzers (Testo, Sparta, NJ, USA). These analyzers use electrochemical sensors to measure the concentration of CO in the fume hood exhaust gas at a sample rate of 1 Hz. The Testo 335 and Testo 350 were spanned to measure concentrations up to 500 ppm and 10,000 ppm, respectively, using calibration gases. The Testo 335 was used when the maximum CO concentration measured during the test was anticipated to be below 500 ppm to provide higher resolution at lower concentrations. The Testo 350 was used when the maximum concentration was anticipated to be above 500 ppm to provide more accurate readings at higher concentrations. After the Testo 350 was spanned to read 10,000 ppm, the analyzer was connected to a bottle of calibration gas with a CO concentration of 101 ppm to assess how accurately it would read lower concentrations. The analyzer read the concentration of CO in the calibration gas with an accuracy of +/- 5 ppm. Multiple steps were taken to ensure that the readings from the electrochemical sensors were accurate. Both the Testo 335 and Testo 350 were recalibrated regularly using calibration gases. In addition, one test was conducted in which CO concentrations were simultaneously measured using the Testo 335 and a Siemens non-dispersive infrared (NDIR) spectrometer (Siemens, Ultramat 6, Munich Germany). The difference between the two measurements was less than 3%.

Real-time temperature data were acquired at 1 Hz from 17 to 24 type K thermocouples (Omega Engineering, Inc., Stamford, CT USA) installed on each stove. Gas temperature measurements included inlet air temperature, preheated secondary air temperature, and exhaust gas temperature. Temperatures were also recorded at various locations in the fuel chamber and on the outside of the stove body. Thermocouple data were acquired by a National Instruments cRIO-9072 chassis that contained one NI 9213 thermocouple input card and two NI 9211 thermocouple input cards. The temperature data were logged by a LabView program. An additional type K thermocouple submerged in the pot of water recorded the water temperature at 0.6875 Hz. The water temperature data were logged by a second LabView program that also controlled the airflow rate through the fume hood and recorded the starting and ending time for each test.

2.3 Test Matrix

Five configurations of natural draft TLUD semi-gasifier cookstoves were tested (see Figure 2). The first three configurations were based on the same stove ("Stove 1"). Stove 1 was a large stove equipped with a chimney. The stove body was 64 cm tall and weighed 37 kg. The stove was constructed primarily from steel sheet metal of various thicknesses. A refractory material lined the inside of the combustion chamber and the area under the pot. In the configuration termed "Stove 1 with riser," a cylindrical sheet metal duct was added above the secondary burner to direct

the flow of hot gases closer to the bottom of the pot. In the configuration termed "Stove 1 with riser and pot skirt," a pot skirt was added and the chimney inlet was moved from the area under the pot to the side of the pot skirt to force the hot gases to flow around the sides of the pot.

Figure 2. Left to right: Stove 1, Stove 1 with riser, Stove 1 with riser and pot skirt, Stove 2, and Stove 3. Stove 1 was 64 cm tall, weighed 37 kg and was equipped with a chimney. Stove 2 was 30 cm tall and weighed 3.6 kg, Stove 3 was 25 cm tall and weighed 2.7 kg.

Stove 2 was a smaller stove without a chimney. Stove 2 was 30 cm tall, weighed 3.6 kg, and was constructed of various steel alloys. A plastic skirt surrounded the base of the stove. Stove 3 was a small stove without a chimney and was based on an open source natural draft semi-gasifier design (Wendelbo, 2012). Stove 3 was approximately 25 cm tall, weighed 2.7 kg, and was constructed using 23 gauge stainless steel sheet metal.

The stoves were tested with two different fuel types: an agricultural waste fuel and a prepared fuel. The agricultural waste fuel consisted of dried corn cobs obtained from a local farm in Windsor, CO. The prepared fuel consisted of wood pellets made from Lodgepole pine by the Rocky Mountain Pellet Company (Walden, CO USA). The density and heating value of each fuel is shown in Table 1. The lower heating value (LHV) of each fuel was determined by first measuring the higher heating value (HHV) using an IKA C200 Calorimeter System (IKA, Staufen, Germany). The LHV was then calculated using an estimated chemical composition for each fuel obtained from the literature. The HHV of the char produced by each fuel type was also measured. The HHV of the char was used in place of the LHV of the char in all calculations because the chemical composition of the char was unknown. Table 2 contains the matrix of all tests conducted in this study.

Table 1. Bulk density, density, and lower heating value of corn cob and wood pellet fuels

Fuel type	*Bulk density (kg/m^3)*	*Density (kg/m^3)*	*LHV_{daf} (J/g)*
Corn cobs	195 (Coovattanachai, 1989)	340 (Lin et al., 1995)	18,119
Wood pellets	696 (Rocky Mountain Pellet Company, 2012)	1260 ± 55	19,560

Table 2. Matrix of all tests conducted

Configuration	*Fuel type*	*Number of replicates*
Stove 1	Corn cobs	4
Stove 1	Wood pellets	3
Stove 1 with riser	Corn cobs	2
Stove 1 with riser	Wood pellets	3
Stove 1 with riser and pot skirt	Corn cobs	3
Stove 1 with riser and pot skirt	Wood pellets	3
Stove 2	Corn cobs	3
Stove 2	Wood pellets	3
Stove 3	Corn cobs	3
Stove 3	Wood pellets	3

2.4 Efficiency Calculations

In addition to the emissions and temperature measurements described above, efficiency measurements were made for each of the design configuration/fuel type combinations shown in Table 2. The *heat transfer efficiency* of each stove is defined as the ratio of the energy transferred to the water to the energy *released* via combustion of the fuel. As calculated using Equation 1 (DeFoort et al., 2010), the heat transfer efficiency is a measure of how effectively the heat from the flame and the hot gases is transferred to the pot:

$$\eta_{HT} = \frac{c_{p,H2O} m_{H2O} \Delta T_{H2O} + h_{v,H2O} m_{H2O,evap}}{m_{fuel,dry} LHV_{fuel,daf} - m_{fuel} MC_{fuel} \left(c_{p,H2O} \Delta T_{H2O \in fuel} + h_{v,H2O}\right) - LHV_{char} m_{char}} \quad (1)$$

where $c_{p,H2O}$ is the specific heat of water (J/g-K), m_{H2O} the mass of water boiled during the test (g), ΔT_{H2O} the change in the water temperature between the beginning and end of the test (K), $h_{v,H2O}$ the heat of vaporization of water (J/g), $m_{H2O,evap}$ the mass of water evaporated out of the pot during the test (g), $m_{fuel,dry}$ the dry mass of fuel consumed (g), LHV_{fuel} the dry, ash-free lower heating value of the fuel (J/g),m_{fuel} the wet mass of fuel consumed (g), MC_{fuel} the moisture content of the fuel (as a percentage of mass on a wet basis), $\Delta T_{H2O \in fuel}$ the temperature change that the water in the fuel had to undergo before it was evaporated (assumed to be 75 K), LHV_{char} the lower heating value of the charcoal produced from the fuel (J/g), and m_{char} the mass of the ash and charcoal remaining at the end of the test (g).

The *overall efficiency* of each stove is defined as the ratio of the energy transferred to the water to the energy available in the dry mass of fuel consumed (Equation 2). In this formulation, the energy remaining in the charcoal left at the end of the test represents an energy loss. Although this energy is still available for subsequent use, it should not be assumed that this chemical energy will be converted into useful thermal energy (Kar et al., 2012). It should be noted, however, that most studies on stove performance do account for the energy remaining in the char and report heat transfer efficiency or "thermal efficiency" using calculations similar to Equation 1 (Jetter and Kariher, 2009, MacCarty et al., 2010).

$$\eta_{OA} = \frac{c_{p,H2O} m_{H2O} \Delta T_{H2O} + h_{v,H2O} m_{H2O,evap}}{m_{fuel,dry} LHV_{fuel,daf}} \quad (2)$$

2.5 Energy Balance Calculations

To determine the greatest sources of efficiency loss and to inform future design efforts, all of the energy sources and energy transfers present during stove operation are accounted for in a thermodynamic energy balance model. The sources of energy include the energy in the fuel and the energy in the inlet air. The energy transfers include the energy transferred to the water, the energy contained in the char remaining at the end of the test, the energy transferred to and stored in the stove body, the energy lost through convection and radiation heat transfer from the outside of the stove body to the surroundings, and the energy lost through the exhaust gases.

The energy contained in the fuel is calculated using Equation 3:

$$E_{fuel} = m_{fuel,dry} LHV_{fuel,daf} \quad (3)$$

whereE_{fuel} is the energy contained in the fuel (J),$m_{fuel,dry}$ the dry mass of fuel consumed during the test (g), and LHV_{fuel} the dry, ash-free lower heating value of the fuel (J/g).

The energy transferred to the water is calculated using Equation 4:

$$E_{H2O} = c_{p,H2O} m_{H2O} \Delta T_{H2O} + h_{v,H2O} m_{H2O,evap} \quad (4)$$

where E_{H2O} is the energy transferred to the water (J), $c_{p,H2O}$ is the specific heat of water (J/g-K), m_{H2O} the mass of water boiled during the test (g), ΔT_{H2O} the change in the water temperature between the beginning and end of the test (K), $h_{v,H2O}$ the heat of vaporization of water (J/g), $m_{H2O,evap}$ the mass of water evaporated out of the pot during the test (g).

The energy contained in the char remaining at the end of the test is calculated using Equation 5:

$$E_{char} = m_{char} HHV_{char} \tag{5}$$

where E_{char} is the energy contained in the char (J), m_{char} the mass of char (g), and HHV_{char} the higher heating value of the charcoal (J/g). As mentioned above, the higher heating value of the char is used because the chemical composition of the char is unknown.

For Stoves 2 and 3, the energy added to the stove body is calculated by multiplying the mass of the stove by the specific heat of the metallic stove body and the change in the temperature of the stove body between the beginning and end of the test (Equation 6).

$$E_{stove} = m_{stove} c_{p,stove} \Delta T_{stove} \tag{6}$$

where E_{stove} is the energy stored in the stove body (J), m_{stove} the mass of the stove (kg), $c_{p,stove}$ is the specific heat of the material the stove is constructed from, and ΔT_{stove} the change in the temperature of the stove body over the length of the test (K). The plastic skirt around the base of Stove 2 is neglected. The specific alloys that Stoves 2 and 3 are constructed from are unknown and properties of plain carbon steel and AISI 304 stainless steel are assumed for these calculations.

Calculating the amount of energy stored in the body of Stove 1 is more complicated because, although the structure of the stove is composed primarily of steel, the stove body contains a large mass of dense refractory material. The larger thickness and lower thermal conductivity of the refractory material (in comparison to the steel) makes a heat transfer model for determining the amount of thermal energy stored in the refractory material during the test necessary. The steel stove body accounts for approximately 2/3 of the total mass of the stove. The energy stored in the steel portion is calculated using Equation 6. A large mass of refractory lining between the secondary burner and the pot accounts for the other 1/3 of the stove's mass. The area under the pot consists of a cylindrical cavity with a diameter of 31 cm and a height of 11 cm. A block of refractory material fills the area between this cavity and the outside of the stove and has a total volume of 6,270 cm^3.

The temperature of the steel walls on the outside of the stove and the temperature of the hot gases passing through the cavity under the pot are known. The temperature profile within the block of refractory material is estimated using a thermal resistance model. The resistance elements include convection between the hot gases and the inside walls of the refractory block, conduction through the refractory block, and conduction through the steel wall of the stove. Although the inside wall of the block is circular and the outside is a square, conduction through the block is modeled as if the block were a cylindrical ring with a volume equivalent to its actual volume. The steel wall is also modeled as cylindrical with the same thickness as the actual steel wall.

For the original geometry of Stove 1, convection heat transfer to the inside wall is modeled as natural convection over a vertical plate because the diameter of the cavity is large. It is assumed that the temperature of the inside wall of the refractory block does not vary with position over the height of the block. The Nusselt number correlation developed by Churchill and Chu for convection over an isothermal, vertical flat plate when the Rayleigh number is less than 10^9 (Incropera et al., 2007, Churchill and Chu, 1975) is used (Equation 7).

$$\overline{Nu}_L(t) = \frac{0.68 + 0.670 Ra_L(t)^{1/4}}{[1 + (0.492/Pr)^{9/16}]^{4/9}} \tag{7}$$

where $\overline{Nu}_L(t)$ is the average Nusselt number over the entire length of the plate as a function of time, Ra_L the Rayleigh number as a function of time, and Pr is the Prandtl number.

For the remaining cases where the riser or the riser and pot skirt are used, convection is modeled as natural convection inside of an annulus where the inner wall of the annulus is hot and the outer wall of the annulus is cold [19]. For these cases, the Nusselt number correlation developed by Nagendra et al. (1970) is used (Equation 8) (Nagendra et al., 2007, Martynenko and Khramtsov, 2005).

$$\overline{Nu}_L(t) = \frac{0.48Ra_L(t)}{6830(L/d_2)^4(d_1/L) + Ra_L(t)^{3/4}} \quad \text{where } (L/d_1)Ra_L(t)^{-1/4} < 0.1 \tag{8}$$

where $\overline{Nu}_L(t)$ is the average Nusselt number as a function of time, $Ra_L(t)$ the Rayleigh number as a function of time, L the length over which the heat transfer takes place (m), d_2 the diameter of the outer cylinder (m), and d_1 the diameter of the inner cylinder (m).

The Rayleigh number, Nusselt number, convection coefficient, heat transfer through the block, and inner wall temperature of the block are recalculated at every time step. The Rayleigh number is calculated using the inner wall temperature calculated for the previous time step. Once the final inner wall temperature and final heat transfer through the block are calculated, the total amount of energy stored in the refractory block at the end of the test is calculated using Equation 9.

$$E_{stored} = \rho c_{p,refractory} 2\pi L \int_{r_1}^{r_2} \left[\left(T_{inner,f} - \frac{Q_f ln(r/r_1)}{2\pi kL} \right) - T_i \right] r dr \tag{9}$$

where E_{stored} is the amount of energy stored in the block of refractory material (J), ρ the density of the refractory material (kg/m^3), $c_{p,refractory}$ the specific heat of the refractory material (J/kg-K), L the height of the refractory block (m), T_i the initial temperature of the stove body (K), $T_{inner,f}$ the temperature of the inner wall of the block at the last time step (K), Q_f the heat transfer through the block at the last time step (W) , k the thermal conductivity of the refractory material (W/m-K), r the radius of the block (m), r_1 the inner radius of the block (m), and r_2 the outer radius of the block (m). The refractory material is assumed to have properties similar to those of cement mortar (Incropera et al., 2007).

The heat lost through convection from the stove body is calculated using Equation 10:

$$E_{conv} = \int_0^{t_f} h(t)A(T(t) - T_\infty)dt \tag{10}$$

where E_{conv} is the energy lost through convection (J), $h(t)$ the convection coefficient as a function of time (W/m^2-K), A the surface area of the sides of the stove (m^2), $T(t)$ the temperature of the stove body as a function of time (K), T_∞ the temperature of the surroundings (K) , and t_f the length of the test (s).

Equation 10 is integrated numerically using the outside stove body temperature that is recorded every second during the tests as $T(t)$. Rayleigh number, Nusselt number, and the convection coefficient are recalculated at every time step. The average of the primary and secondary air inlet temperatures at time 0 is taken as the ambient air temperature.

The outside of Stove 1 is modeled as 4 vertical plates. The outside wall of Stoves 2 and 3 are modeled as a single vertical plate with a surface area equal to the surface area of the cylindrical outside wall. The convection coefficient, *h*, is calculated using the Nusselt number correlation for natural convection over an isothermal vertical plate shown in Equation 7. It is assumed that the outside walls are isothermal at each time step.

The heat lost through radiation from the stove body is calculated using Equation 11:

$$E_{rad} = \int_0^{t_f} \epsilon\sigma A\left(T(t)^4 - T_\infty{}^4\right)dt \tag{11}$$

where E_{rad} is the energy lost through radiation (J), ϵ the emissivity of the stove, σ the Stefan-Boltzmann constant (W/m^2-K^4), A the surface area of the stove (m^2), $T(t)$ the temperature of the stove body as a function of time (K), and T_∞ the temperature of the surroundings (K). Equation 12 is integrated numerically using the same temperatures used in Equation 10.

The total amount of energy transferred to the water, contained in the char at the end of the test, stored in the stove body, and lost through radiation and convection from the outside walls of the stove is subtracted from the total energy contained in the fuel input at the beginning of the test. The difference is the amount of energy lost through the exhaust from the stove.

3. Results and Discussion

The emissions and heat transfer efficiencies measured during each test, as well as the results of the thermodynamic energy balance model, are given below.

3.1 EPTP Results

The measured CO and PM_{10} emissions from all 5 stove configurations, shown in Figure 3, varied substantially with fuel type. In general, the measured emissions from all stoves were lower when wood pellets were used as fuel instead of corn cobs. For example, when the baseline configuration of Stove 1 was fueled with wood pellets instead of corn cobs, CO emissions decreased by a factor of 47 and PM_{10} emissions decreased by a factor of 6. Similarly, when Stove 2 was fueled with wood pellets instead of corn cobs, CO emissions decreased by a factor of 2. When Stove 3 was fueled with wood pellets instead of corn cobs, CO emissions decreased by a factor of 11 and PM_10 emissions decreased by a factor of 3.

Although the design changes made to Stove 1 were effective in reducing emissions, Stove 1 generally produced much higher emissions than both Stoves 2 and 3. Stove 3 exhibited the lowest emissions overall. As shown in Figure 4, Stoves 2 and 3 were also more efficient than Stove 1. Unlike emissions, heat transfer efficiency was not affected by fuel type.

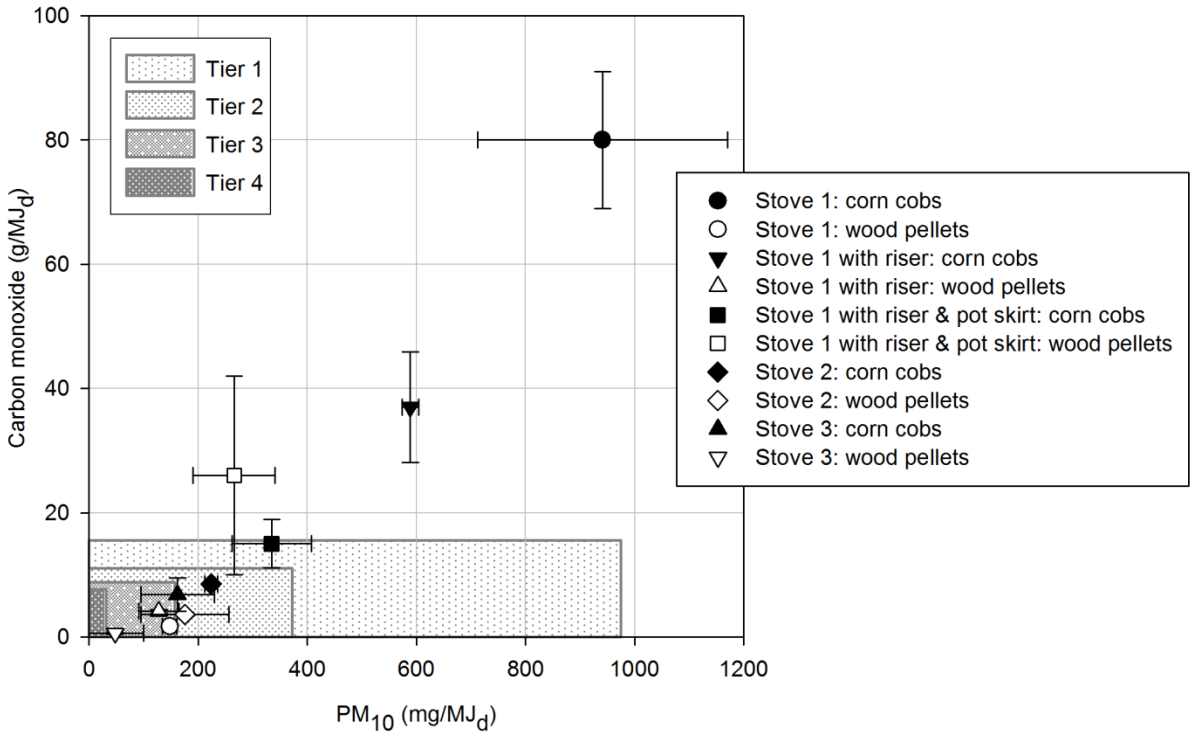

Figure 3. High power carbon monoxide emissions vs. high power particulate matter emissions compared to ISO tiers for high power biomass stove performance.

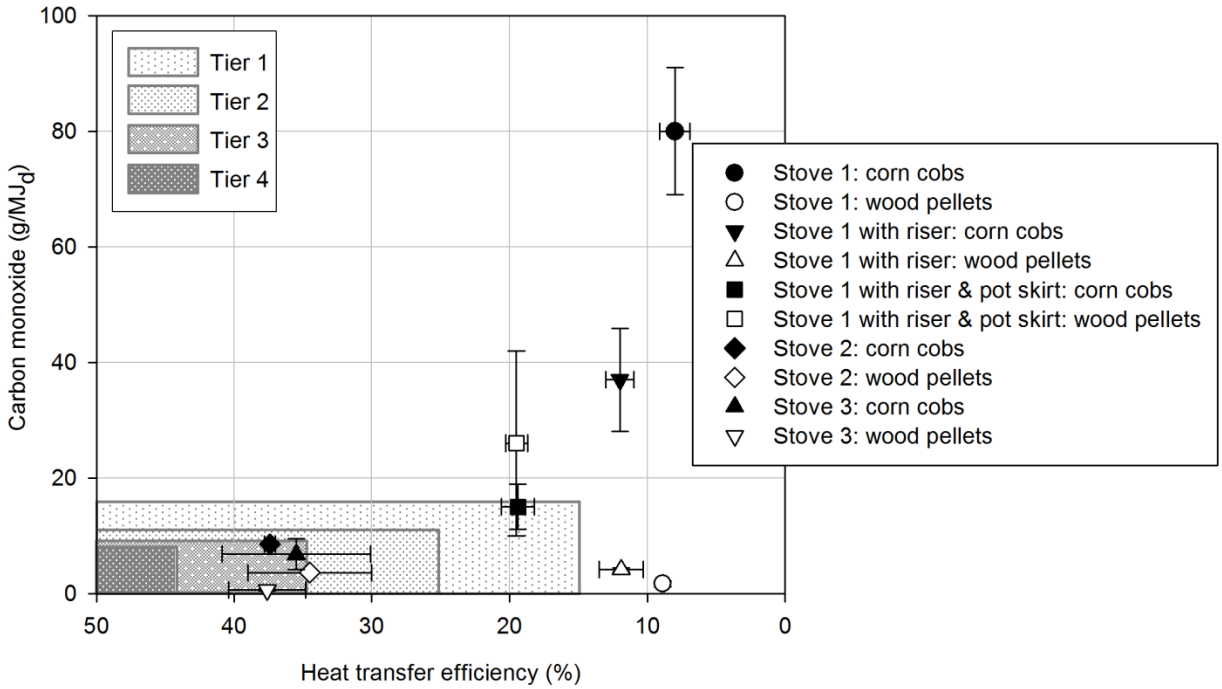

Figure 4. High power carbon monoxide emissions vs. heat transfer efficiency compared to ISO tiers for high power biomass stove performance

In Figures 3 and 4, the performance of each stove has been compared to the standards for high power performance provided in the ISO standards for biomass cookstoves (ISO International Workshop on Clean and Efficient Cookstoves, 2012). The ISO standards describe a tiered system for rating high power performance in terms of CO emissions, PM emissions, and efficiency. For each parameter, 5 levels of performance ranging from Tier 0 to Tier 4 are included (ISO International Workshop on Clean and Efficient Cookstoves, 2012). Tier 0 represents a stove that is comparable to or worse than a three stone fire or traditional stove. Tier 4 represents a very highly performing stove that would be expected to decrease health risks substantially. Tiers 1 through 3 represent various levels of improved stoves.

In terms of these tier ratings, Stove 1 had the most variable performance, which ranged from Tier 0 to Tier 3, depending on the fuel type and design configuration implemented. The performance of Stove 2 was the least variable; emissions remained within Tier 2 for both fuel types. Emissions from Stove 3 were on the border between Tier 2 and Tier 3 when the stove was fueled with corn cobs and on the border between Tier 3 and Tier 4 when the stove was fueled with wood pellets (Figure 3). It should also be noted that although several of the configuration/fuel combinations met Tier 4 standards in terms of CO, only Stove 3/wood pellets came close to meeting Tier 4 PM_{10} standards. These results do suggest, however, that natural draft TLUD semi-gasifier cookstoves have the potential to meet Tier 4 emissions standards. As shown in Figure 4, meeting Tier 4 heat transfer efficiency standards might be more problematic.

The two design changes made to Stove 1 were motivated by the very low efficiencies measured for the original configuration. The efficiency increased substantially when the riser and pot skirt were added. The effects of these design changes on CO and PM_{10} emissions varied depending on the fuel type. Specifically, when Stove 1 was fueled with corn cobs, emissions decreased substantially when the riser and pot skirt were added. When Stove 1 was fueled with wood pellets, however, the CO and PM emissions actually increased when the riser and pot skirt were added (Figure 4).

The very high CO emissions observed when Stove 1 was operated in its original configuration using corn cob fuel resulted from the need to refuel the stove prior to completion of the EPTP due to the low bulk energy content in the corn cobs and high thermal mass of the stove. This determination was made by comparing real-time CO measurements with real-time temperature measurements taken inside the fuel chamber. Fuel bed temperature measurements allowed tracking of the primary combustion zone during stove operation. The data from a representative cold start test performed with the original stove geometry and corn cob fuel is shown in Figure 5a. Emissions levels were lowest at the beginning

of the test just after ignition when gasification had not yet started. Emissions became noticeably higher once gasification started. Emissions increased once again when the entire fuel bed had gasified and the char began to burn. After the char was burnt, fuel had to be added to continue the test. Subsequent batches of fuel were consumed very quickly and emissions became higher than at any other point during the test. During these times the stove was no longer operating purely as a TLUD semi-gasifier.

Similar emissions trends were observed when Stove 1 was operated in the two modified configurations using corn cob fuel. The modifications did not reduce CO emissions levels for the first batch of fuel substantially. However, because the modifications improved the heat transfer to the pot, thereby decreasing the time to boil, the stove was refueled fewer times. The lower overall emissions for the entire tests were the result of reducing the number of emissions spikes. With the addition of the riser, consumption of the original batch of corn cob fuel proceeded more slowly than in the baseline configuration and the stove only had to be refueled once during the test (Figure 5c). With the addition of the riser *and* pot skirt, the approximate time to boil was reduced from 25 to 15 minutes and the stove did not have to be refueled during the test (Figure 5e).

When Stove 1 was fueled with wood pellets, extremely low CO emissions were observed for the baseline configuration (Figure 5b). In this case, Stove 1 did not require refueling prior to completion of the test. Emissions were not affected substantially by the addition of the riser (see Figures 5b and 5d). However, emissions levels increased substantially when the riser and pot skirt were added (Figure 5f). In this configuration, enhanced heat transfer from the hot gases to the pot may have actually limited the oxidation of pollutants by reducing the gas temperature.

The performance of Stove 2 did not vary as substantially with fuel type as the performance of Stove 1 varied. The CO emissions, shown in Figure 6, were slightly higher when the corn cob fuel was used. Stove 2 had to be refueled once during the cold start when corn cobs were used and emissions spiked upon refueling. However, these spikes were not as dramatic as those observed with Stove 1.

Stove 3 did not require refueling during the cold start for either of the fuels (Figure 7). When Stove 3 was operated with wood pellets, only a small portion of the fuel chamber had to be filled to complete the test. However, when Stove 3 was operated with corn cobs the fuel chamber was filled completely.

The results of the cold start testing with the two different fuel types illustrate how the bulk energy density of the fuel and thermal mass of the stove impact the CO emissions and heat transfer efficiency. It is understood that the choice of fuel type used in the field is dictated by cost and availability; however, the results underscore the need to know the fuel type so that it can be incorporated into the stove design for TLUD semi-gasifier cookstoves. Moreover, stove dissemination must be accompanied by training to educate users on the issues associated with adding fuel onto the hot char bed.

Because only the cold start phase of the EPTP was completed, the results do not provide a complete picture of the performance of each stove. The results of the hot start phase are also typically considered when evaluating high power performance. The ISO standards for biomass cookstoves also include emissions and efficiency standards for low power operation (ISO International Workshop on Clean and Efficient Cookstoves, 2012). However, the purpose of this study was not to provide a comprehensive review of stove performance; instead, the purpose was to provide a comparison between three different stoves all designed around the same natural draft TLUD semi-gasifier operating principle.

It should also be noted that all three stoves exhibited emissions spikes during shut-down. These spikes are not shown in Figures 5 through 7, however, because emissions from the shut-down process are not included in the EPTP or any other water boiling test. However, the existence of shut-down emissions, as well as mitigation methods, should be considered since users will be exposed to these emissions during real-world use of semi-gasifier cookstoves.

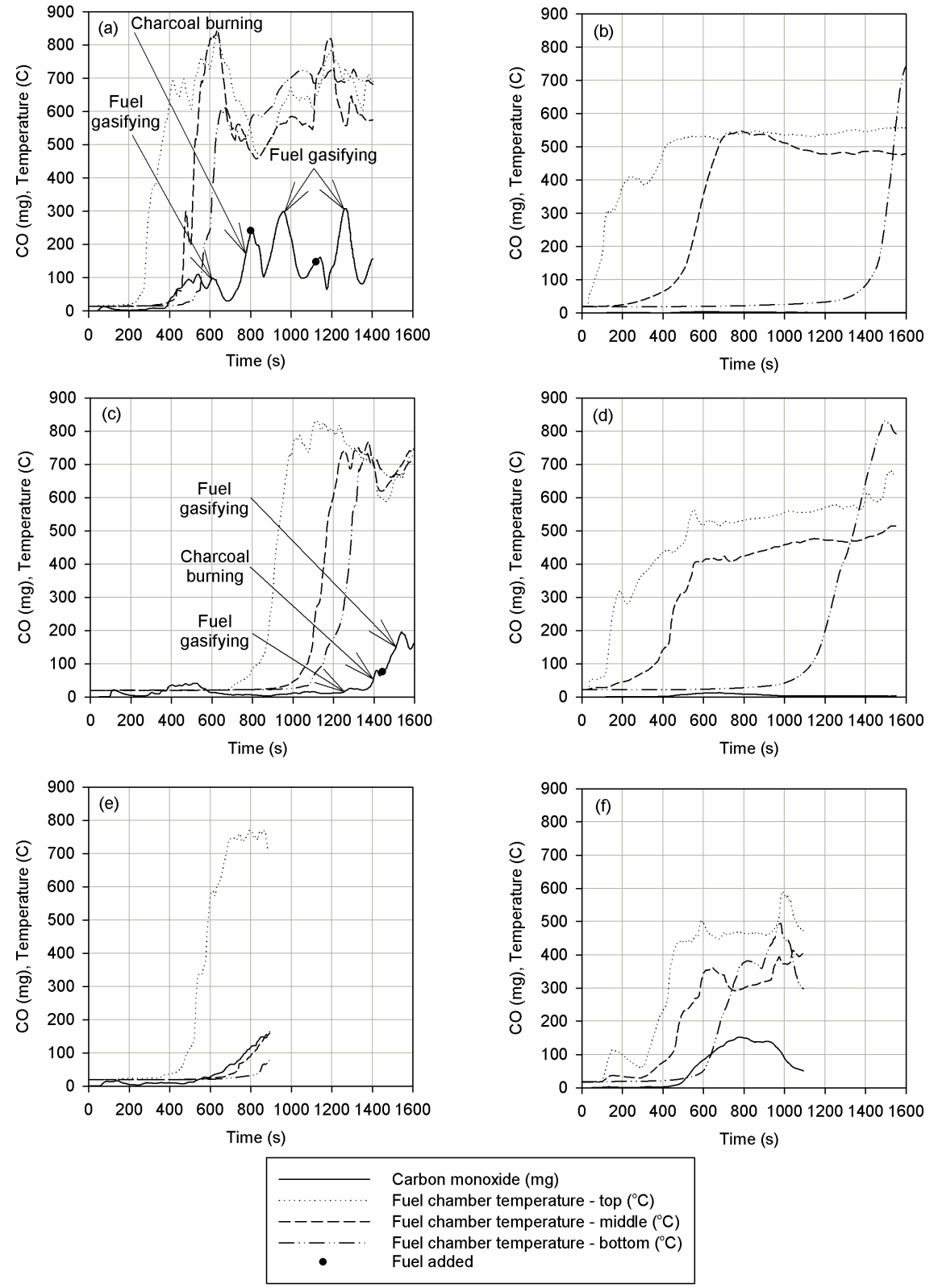

Figure 5. CO emissions and fuel chamber temperatures during a cold start test done using Stove 1 (a) in its baseline configuration with corn cob fuel, (b) in its baseline configuration with wood pellet fuel, (c) with the riser and corn cob fuel, (d) with the riser and wood pellet fuel, (e) with the riser and pot skirt and corn cob fuel, and (f) with the riser and pot skirt and wood pellet fuel.

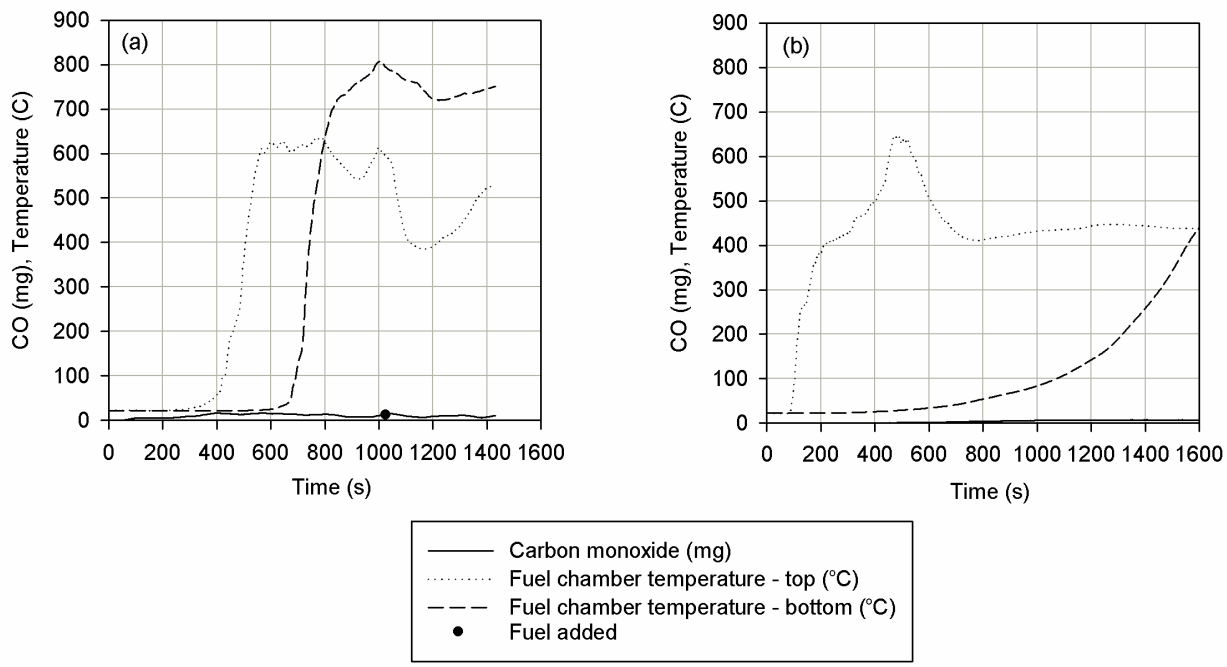

Figure 6. CO emissions and fuel chamber temperatures during a cold start test done using Stove 2 (a) with corn cob fuel and (b) with wood pellet fuel.

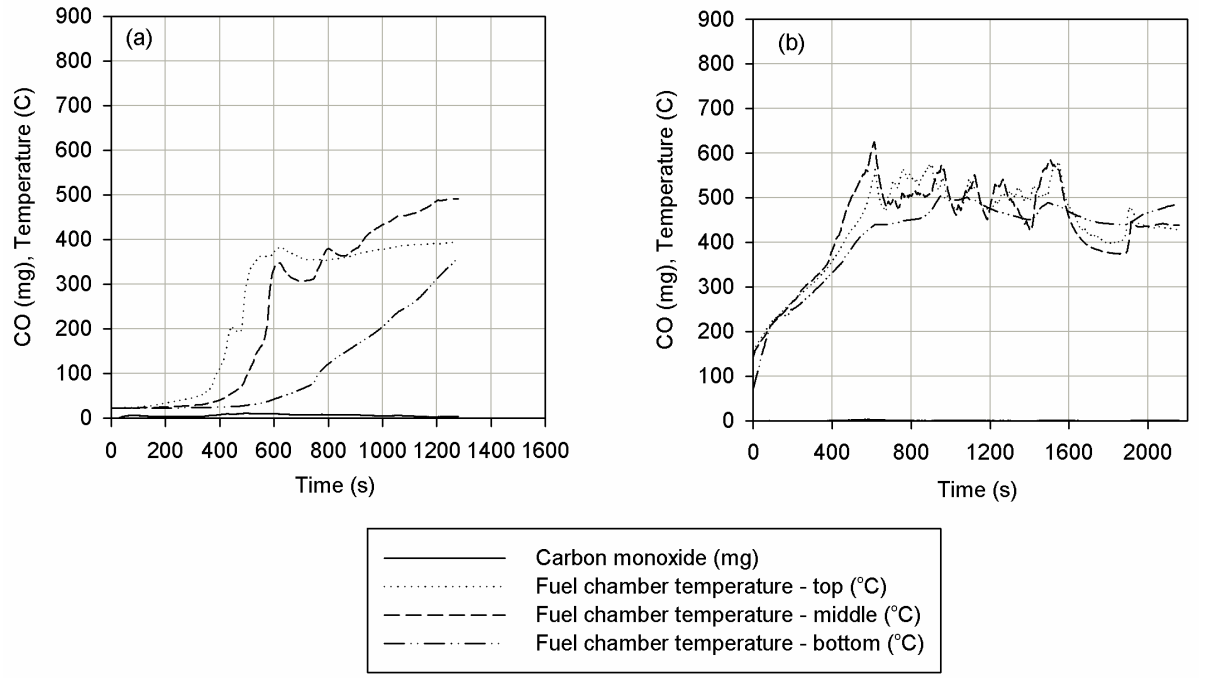

Figure 7. CO emissions and fuel chamber temperatures during a cold start test done using Stove 3 (a) with corn cob fuel and (b) with wood pellet fuel.

3.2 Energy Balance Results

The results of the energy balance model are illustrated in Figures 8 and 9. The calculated quantities of energy transferred to the water and stove body; remaining in the char; and transferred out of the stove via the exhaust gases, convection and radiation are shown. For each stove/fuel combination, the results are reported in terms of total energy (Figure 8) and as a fraction of the total energy contained in the fuel that was consumed (Figure 9).

Stove 1 used the greatest amount of energy to complete the test (Figure 8). Compared to the other two stoves, Stove 1 had more heat addition to the stove body and energy transferred out of the stove via the exhaust gases. These larger losses were the result of the high thermal mass of Stove 1 and the presence of the chimney [11]. The heat transfer efficiency of a cookstove is dependent upon the ability to transfer heat to the cooking surface through radiation from the flame and convection from the hot gases. The amount of heat transferred to the cooking surface by convection is proportional to the area over which the hot gases flow. The original configuration of Stove 1, as well as the configuration with the addition of the riser, only allowed heat to be transferred to the pot by radiation and by hot gases impinging on the bottom of the pot. The surface area for convection was limited to the area of the bottom of the pot. Consequently, the heat transfer efficiencies were low in these configurations. The configuration with the riser and pot skirt increased the area over which convective heat transfer to the pot occurred by forcing the hot gases to flow around the sides of the pot. It should be noted that a faster time to boil also resulted in reduced energy losses due to stove body heating, despite the high thermal mass of Stove 1, as evidenced by the results for the configuration with the riser and pot skirt fueled with corn cobs.

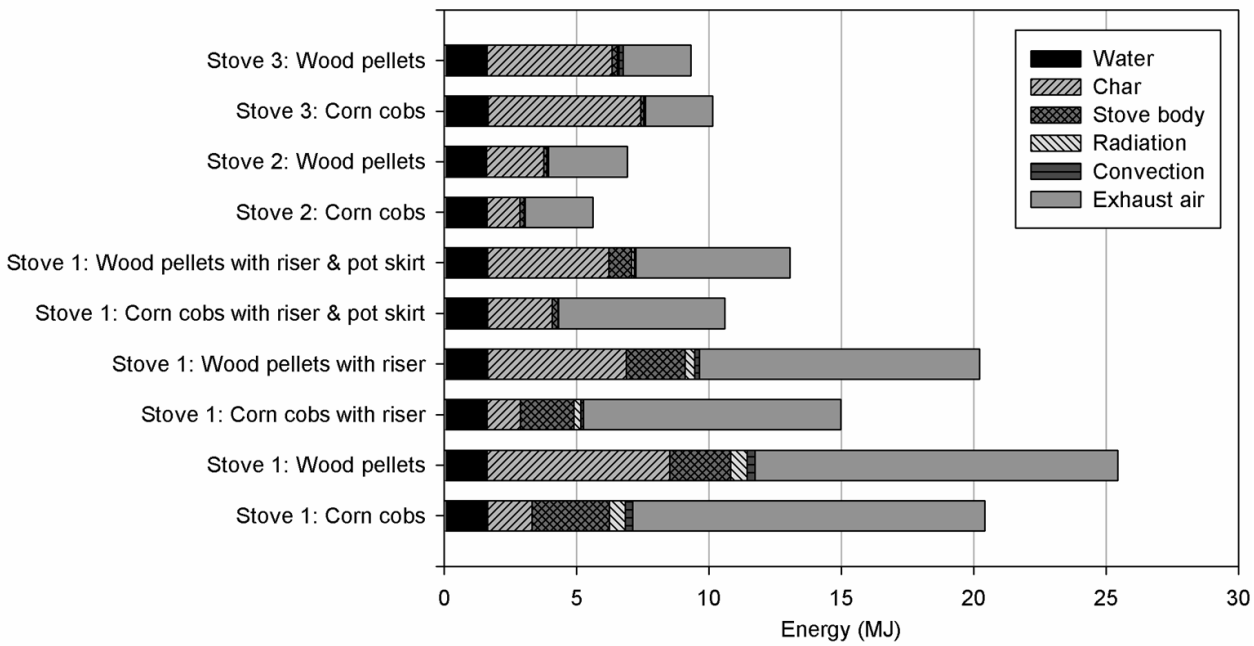

Figure 8. Results of the energy balance with the total energy consumption attributed to each component shown.

When a semi-gasifier stove is evaluated, it is important to consider the difference between the heat transfer efficiency of the stove and the overall efficiency of the stove. Although the heat transfer efficiencies of Stoves 2 and 3 were comparable (Figure 4), Stove 3 used more energy to complete the test than Stove 2 (Figure 8). This difference was due to the fact that a large amount of the energy input to Stove 3 was left over as char at the end of the test (Figure 9). Although the average heat transfer efficiency of Stove 3 was approximately 35%, the average overall efficiency was only 16% (Figure 9). If the char left over at the end of the test is put to some use (for example, as a fuel in a charcoal-burning stove or as a soil amendment), the low overall efficiency may not be a disadvantage to the stove user. For Stoves 2 and 3, which had lower thermal mass because of their smaller size and lack of refractory lining, energy losses due to stove body heating, convection from the stove body to the ambient air, and radiation from the stove body were all very low (Figure 8).

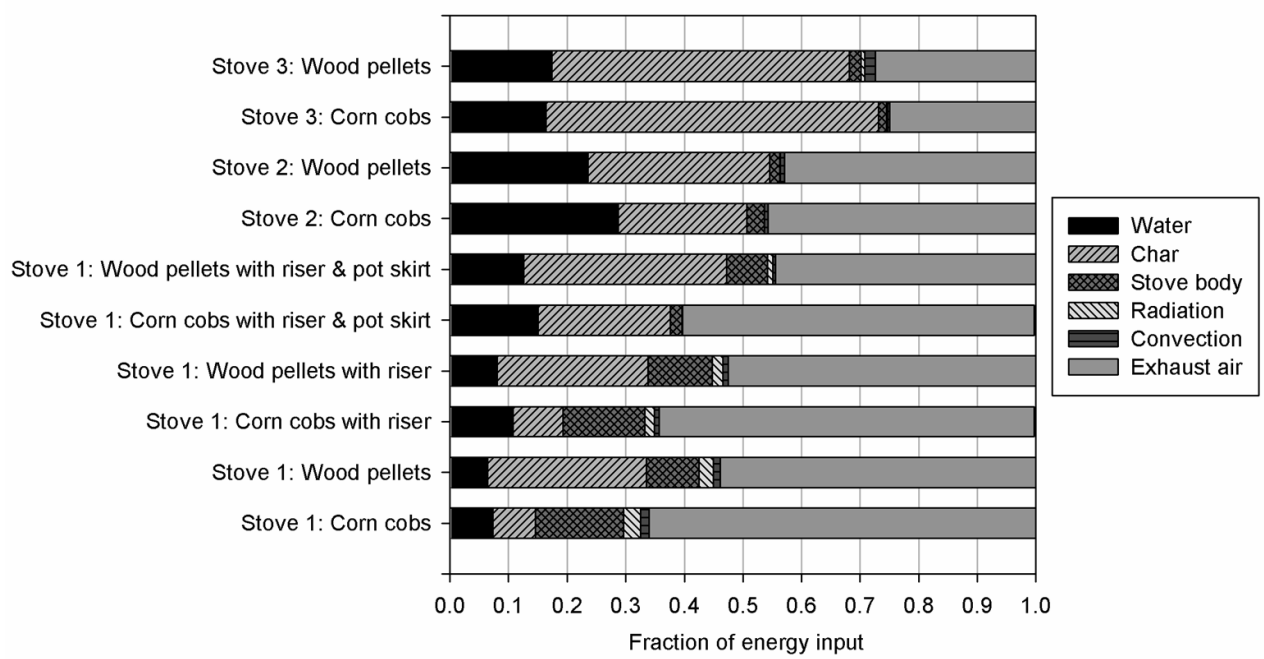

Figure 9. Results of the energy balance with the total energy consumption attributed to component shown as a percentage of total energy consumption.

4. Conclusions

The results of this study suggest that there is a wide variation in performance among different natural draft TLUD semi-gasifier cookstoves. The type of fuel used has a profound effect on the exhaust emissions, but the magnitude of this effect is largely governed by the bulk energy content of the initial fuel loading and the efficiency at which this energy is transferred to the water. The results show that natural draft TLUD semi-gasifier cookstoves do have the potential to achieve low emissions when operated under controlled conditions (specified fuel type and operating procedure). Additional work is needed to develop a natural draft gasifier cookstove that meets ISO Tier 4 performance standards, but the results of this study suggest that Tier 4 emissions may be readily achievable in this relatively simple design. Achieving Tier 4 heat transfer efficiency, however, may require substantially more research and development.

The instantaneous CO and temperature measurements strongly suggest that refueling TLUD semi-gasifier cookstoves results in CO emissions spikes. In the field, there is no guarantee that users will refrain from refueling the stove during operation and thereby be exposed to these CO emissions spikes. Improving the heat transfer efficiency of a stove can reduce the incidence of these spikes by increasing the amount of useful energy that can be delivered to the cooking surface without refueling. However, eliminating these spikes altogether by developing a stove design that can respond to transient conditions will be necessary to ensure low CO emissions in the field. Eliminating the high emissions that are observed when the stove is shut down and/or switches from gasification mode to char combustion mode would also be required.

Stoves should be tested in the laboratory using all fuels that may be used in the field. Existing TLUD semi-gasifier cookstove designs should not be promoted as capable of utilizing any biomass as fuel. Although the stove will function using a wide variety of fuels, emissions performance will vary substantially. This study clearly shows that TLUD semi-gasifier cookstoves that exhibit very low emissions with one fuel type may exhibit very high emissions with another fuel type. Accordingly, further research and development efforts must be aimed at developing cookstove designs whose emissions and performance are agnostic to the solid biomass fuel source.

Acknowledgements

The authors acknowledge the National Science Foundation for providing a graduate research fellowship to Jessica Tryner (NSF DGE 0801707). The authors also acknowledge Impact Carbon for funding a portion of the experiments.

References

Anderson, P. S., Reed, T. B., and Wever, P. W. (2007). Micro-gasification: What it is and why it works. *Boiling Point*, **53**, 35.

Bruce, N., Rehfuess, E., Mehta, S., Hutton, G., and Smith, K. (2006). Indoor air pollution. In Jamison, D. T., Breman, J. G., Measham, A.R., Alleyne, G., Claeson, M., Evans, D.B., et al. (Eds.) *Disease Control Priorities in Developing Countries (2nd Edition)*, Oxford University Press, New York, Chap. 42. pp. 793-815.

Churchill, S.W., and Chu, H. H. S. (1975). Correlating equations for laminar and turbulent free convection from a vertical plate. *International Journal of Heat and Mass Transfer*, **18**, 1323.

Coovattanachai, N. (1989). Biomass gasification research and field experiments by the Prince of Songkla University, Thailand. *Biomass*, **18**, 241.

DeFoort, M., L'Orange, C., Kreutzer, C., Lorenz, N., Kamping, W., and Alders, J. (2010). Stove Manufacturers Emissions and Performance Test Protocol (EPTP). Engines and Energy Conversion Laboratory, Colorado State University, Fort Collins, C.O.

Goldemberg, J., Johansson, T. B., Reddy, A. K. N., Williams, R. H. (2004). A global clean cooking fuel initiative. *Energy for Sustainable Development*, **8**, 5.

Incropera, F. P., DeWitt, D. P., Bergman, T. L., and Lavine, A. S. (2007). *Fundamentals of Heat and Mass Transfer, 6th ed*. John Wiley and Sons, Hoboken.

ISO International Workshop on Clean and Efficient Cookstoves. (2012). Available at: http://www.pciaonline.org/files/ISO-IWA-Cookstoves.pdf.

Jetter, J. J., and Kariher, P. (2009). Solid-fuel household cook stoves: Characterization of performance and emissions. *Biomass and Bioenergy*, **33**, 294.

Kar, A., Rehman, I. H., Burney, J., Praveen Puppala, S., Suresh, R., Singh, L., Singh, V. K., Ahmed, T., Ramanathan, N., and Ramanathan, V. (2012). Real-time assessment of black carbon pollution in Indian households due to traditional and improved biomass cookstoves. *Environmental Science and Technology*, **46**, 2993.

Lin, J. L., Keener, H. M., Essenhigh, R. H. (1995). Pyrolysis and combustion of corncobs in a fluidized bed: measurement and analysis of behavior. *Combustion and Flame*, **100**, 271.

L'Orange, C., DeFoort, M., and Willson, B. (2012). Influence of testing parameters on biomass stove performance and development of an improved testing protocol. *Energy for Sustainable Development*, **16**, 3.

MacCarty, N., Still, D., and Ogle, D. (2010). Fuel use and emissions performance of fifty cooking stoves in the laboratory and related benchmarks of performance. *Energy for Sustainable Development*, **14**, 161.

Martynenko, O. G., and Khramtsov, P. P. (2005). *Free-Convective Heat Transfer: With Many Photographs of Flows and Heat Exchange.* Springer, New York.

Nagendra, H. R., Tirunarayanan, M. A., and Ramachandran, A. (1970). Free convection heat transfer in vertical annuli. *Chemical Engineering Science*, **25**, 605.

Quaak, P., Knoef, H., and Stassen, H. (1999). *Energy from Biomass: A Review of Combustion and Gasification Technologies.* World Bank, Washington, D.C.

Reed, T. B., and Larson, R. (1996). A wood-gas stove for developing countries. *Energy for Sustainable Development*, **3**, 34.

Rehfuess, E., Mehta, S., and Prüss-Üstün, A. (2006). Assessing household solid fuel use: multiple implications for the millennium development goals. *Environmental Health Perspectives*, **114**, 373.

Rocky Mountain Pellet Company, Inc. (2012). Available at: www.rockymountainpellets.com

Smith, K. R. (2010). What's cooking? A brief update. *Energy for Sustainable Development*, **14**, 251.

Smith, K. R., and Balakrishnan, K. (2009). Mitigating climate, meeting MDGs, and moderating chronic disease: The health co-benefits landscape. In *Commonwealth Health Ministers' Update*, Pro-Book Publishing Limited, Woodbridge, Chap. 4. pp. 59-65.

Smith, K. R., and Peel, J. L. (2010). Mind the gap. *Environmental Health Perspectives*, **118**, 1643.

Wendelbo, P., 2012, "The Peko Pe Biomass Household Energy Program," available at: http://wendelborecho.wordpress.com/2012/05/10/downloads, accessed November 29, 2012.